Journal of
Marine Science and Engineering

MDPI

Article

Hybrid Optimized Fuzzy Pitch Controller of a Floating Wind Turbine with Fatigue Analysis

Carlos Serrano [1], Jesus-Enrique Sierra-Garcia [2] and Matilde Santos [3,*]

[1] Dpto. Computer Architecture and Automatic Control, Faculty of Computer Sciences, Complutense University of Madrid, 28040 Madrid, Spain
[2] Electromechanical Department, University of Burgos, 09006 Burgos, Spain
[3] Institute of Knowledge Technology, University Complutense of Madrid, 28040 Madrid, Spain
* Correspondence: msantos@ucm.es

Abstract: Floating offshore wind turbines (FOWTs) are systems with complex and highly nonlinear dynamics; they are subjected to heavy loads, making control with classical strategies a challenge. In addition, they experience vibrations due to wind and waves. Furthermore, the control of the blade angle itself may generate vibrations. To address this issue, in this work we propose the design of an intelligent control system based on fuzzy logic to maintain the rated power of an FOWT while reducing the vibrations. A gain scheduling incremental proportional–derivative fuzzy controller is tuned by genetic algorithms (GAs) and combined with a fuzzy-lookup table to generate the pitch reference. The control gains optimized by the GA are stored in a database to ensure a proper operation for different wind and wave conditions. The software Matlab/Simulink and the simulation tool FAST are used. The latter simulates the nonlinear dynamics of a real 5 MW barge-type FOWT with irregular waves. The hybrid control strategy has been evaluated against the reference baseline controller embedded in FAST in different environmental scenarios. The comparison is assessed in terms of output power and structure stability, with up to 23% and 33% vibration suppression rate for tower top displacement and platform pitch, respectively, with the new control scheme. Fatigue damage equivalent load (DEL) of the blades has been also estimated with satisfactory results.

Keywords: wind energy; floating wind turbine; pitch control; fuzzy logic; structural fatigue

Citation: Serrano, C.; Sierra-Garcia, J.-E.; Santos, M. Hybrid Optimized Fuzzy Pitch Controller of a Floating Wind Turbine with Fatigue Analysis. *J. Mar. Sci. Eng.* **2022**, *10*, 1769. https://doi.org/10.3390/jmse10111769

Academic Editor: Constantine Michailides

Received: 7 October 2022
Accepted: 13 November 2022
Published: 17 November 2022

1. Introduction

The growing demand for energy in which the world is currently immersed has led to the search for new energy sources that are clean and do not generate carbon residues [1–3]. Among them, wind energy emerges as a promising and efficient alternative. Wind turbines (WTs) can be on land or have offshore foundations. Marine turbines have a number of advantages over land-based turbines, such as no space limitations and more limited impact on the ecosystem. More recently, offshore wind turbines have migrated to deep waters, with floating platforms being a promising, cost-effective, and feasible solution for many countries [4,5].

Floating offshore wind turbines (FOWTs) are massive systems capable of generating large amounts of energy. However, they are subjected to huge mechanical loads, vibrations, and external disturbances that make operation difficult, degrade the electromechanical components, reducing the useful life, and even can compromise stability, and cause damage and safety incidents. Therefore, in order to reduce the maintenance costs and extend the useful life, it is key to develop controllers that stabilize the power and, at the same time, reduce the oscillations of the tower and the platform under different operation conditions.

To make it possible, floating marine turbines are equipped with control systems of the angle of the blades by means of actuators. When the control command is the same for all three blades, this is called collective pitch control (CPC), as opposed to individual blade control (IPC). The purpose of the pitch control is to keep the rotor speed at its rated value. However, this is not an easy task due to the highly nonlinear dynamics of these floating devices. They are subjected to waves, strong winds, currents, ice, etc., so they present interesting challenges from the control point of view [6]. Due to the turbine size and heavy loads, blade angle control not only affects the power output but also influences the structural stability of the floating system [7–9]. That is why it is important to analyze the control response of the system taking into account also the structural variables.

In this work, a CPC approach based on fuzzy logic and optimized by genetic algorithms (GAs) is proposed, in order to achieve the output power target while reducing the vibrations suffered by the floating device, partly caused by the action of the pitch control actuators. To ensure a correct behavior under different wind and wave disturbances, the fuzzy logic controller (FLC) is tuned by genetic algorithms and the tuning parameters associated with each weather condition are stored in a database. The fuzzy approach suits the nonlinear behavior of the system better; on the other hand, the GAs facilitate the adjusting of the FLC parameters and also make it possible to include the twofold objective in the fitness function.

The GA has been chosen to optimize the tuning parameters of the FLC based on some reasons. First, it is a fact that the performance of the wind power system not only depends on the controller structure, but it also depends on the artificial optimization technique used to tune it. Thus, it is reasonable to solve real world problems with already proposed heuristic optimization techniques that have been proved efficient, as it is the case of GAs for FLC. Furthermore, the software that simulates real WTs (FAST) allows connection of the wind turbine model with the toolboxes of Matlab software, that implements several optimization tools including GAs in a simple and easy way. In addition, this work is focused on the fuzzy control of floating wind turbines with the dual objective of reducing the vibrations and achieving a stable nominal output power. These two objectives can be included in the cost function of the GA. In any case, different optimization techniques could have been used for this task and an interesting work would be to analyze how this may affect the WT output power.

Hence, the main contributions of this work can be summarized as follows.

- An intelligent hybrid controller of the blade angle of a barge-type FOWT has been proposed. The control architecture combines a gain scheduling incremental proportional–derivative (PD) fuzzy controller and a fuzzy implementation of the wind speed–pitch relationship. As far as we know, this control scheme for collective pitch control of an FOWT is novel.
- The controller is tuned by a genetic algorithm, which allows definition of a fitness function that includes both maintaining the output power to its maximum value and the reduction of the vibrations of the floating structure. The error of the rotor speed and the tower top displacement have been used in this cost function.
- To ensure the correct behavior under different wind speeds and wave heights, the controller is adjusted for different operation conditions.
- This hybrid intelligent control strategy has been validated and compared with the baseline controller embedded in wind turbine simulation software Fatigue, Aerodynamics, Structures, and Turbulence (FAST) by the National Renewable Energy Laboratory (NREL). The intelligent approach gives smaller power error, fewer vibrations (regarding tower displacement and platform pitch) and lower damage equivalent load (DEL) estimated by the rainflow counting technique.

The article has the following structure: Section 2 introduces some related works. Section 3 briefly describes the theoretical control approach of an FOWT turbine. Section 4 presents the proposed intelligent control architecture. In Section 5, the results are discussed. Finally, conclusions and future work end the paper.

2. Related Works

The control of floating turbines has been approached from different perspectives. Focusing on proposals for collective pitch control, conventional control and particularly enhanced proportional–integral (PI) and proportional–integral–derivative (PID) controllers have been previously used. To mention some examples, a PID controller optimized by the ant colony technique is implemented for vibration control under different types of loads [10]. In [11], a robust proportional–integral (PI) controller is presented; optimal gain scheduling strategy is used to improve pitch control, and support vector regression (SVR) is adopted to represent the strong nonlinear relationship between the PI parameters under different operating conditions. A gain scheduling PI controller is also proposed in [12]; in this case, a reduced liberalized model was used for the design of the controller, with the stability margin as the main design criterion. Wang et al. also use a feedforward PID controller to correct misalignment produced by disturbances in the turbine, with a linearized model of the marine device [13].

Another approach for pitch control is based on optimal controllers; in [14], a linear quadratic regulator (LQR) with a Kalman filter for state and disturbance estimation is implemented. In this case, the authors work with the 5 MW OC3 FOWT, spar-type. They apply a platform controller and wave disturbance reduction. A reduction in power fluctuations, blade pitch activity, and platform oscillations is observed, improving the performance. In another related work, using an LQR controller, the authors showed that it is possible to significantly reduce wave disturbances by reducing the response of the FOWT system to these excitations when a low-order multi-input/multi-output (MIMO) description is considered [15]. They use waves of around 2.5 m. In [16], a linear parameter-varying (LPV) controller is used to build a gain scheduling table that is compared with an LQR controller. It is concluded that the former performs better in terms of vibration reduction, while the latter is better in energy production.

Hybrid control strategies have also been widely used in engineering systems [17–19]. Focusing on the pitch control issue, intelligent control techniques have been hybridized with other techniques [20]. Taking advantage of this synergy, a hybrid control which combines radial basis function (RBF) neural networks with classical PID control was applied to an FOWT in [21]. This controller was validated using the software FAST and was proved superior to the other controllers tested. A similar hybrid structure was applied in [6] to a small turbine with satisfactory results. In [22], a lookup table is combined with an RBF neural network for collective pitch control. The lookup table stores the relationship between the wind and the target pitch angle and the RBF corrects the error deviations. In a previous work of the same authors, neural networks were used to improve a pitch control [9]. In this case, the control structure did not take into account the structural effects of the control as in here, nor in [6], where a hybrid neural network and reinforcement learning control strategy was applied. Indeed, estimation and forecasting based on intelligent techniques have been successfully used in the energy field [8,23–25].

Fuzzy logic has been specifically proved as an efficient tool to design controllers for nonlinear systems, besides being easy to implement [26,27]. For instance, in [28] an adaptive PI control loop is added to a fuzzy logic controller to optimize the control performance of wind turbines, with the objective of decreasing the mechanical fatigue and improving the power efficiency. In [29], wind neuro-estimators are used to improve the performance of a pitch fuzzy controller.

As claimed in [30], the design of a fuzzy system can be considered an optimization problem. Among the different techniques that can be used for the tuning of the parameters, evolutionary algorithms and swarm intelligence have been considered suitable techniques for optimizing fuzzy systems. These heuristic techniques alleviate the tedious and time-consuming task of finding appropriate parameters for the fuzzy system by trial and error.

Furthermore, they have already been applied in renewable system modeling. Specifically, in [31] it is shown how these strategies are applied to hybrid energy system photovoltaic– WT (PV-WT) optimization. In [32], differential evolution optimization is applied to tune the input and output scaling factors of a fuzzy PID controller for a thermal power system. Borni et al. propose fuzzy logic control (FLC) and particle swarm optimization (PSO) algorithms improved using a genetic algorithm (GA) for the control of a wind turbine with a permanent magnet synchronous generator (PMSG) to maximize power generation [33]. In this case, the evolutive FLC tuning procedure alters the membership function mapping to reach the maximum power point tracking (MPPT).

The study proposed by Sharma and Tayal (2022) is focused on achieving the desired rotor speed and frequency control for doubly fed induction generator (DFIG) wind turbines [34]. Among others, they propose a fuzzy logic controller whose scaling parameters have been tuned using a GA. The quantitative comparisons of the control schemes implemented showed that the GA-optimized fuzzy PID controller provides the best frequency control in terms of time-domain specifications. Similarly, Alaoui et al. (2021) propose a fuzzy-based MPPT controller to extract the maximum power point of a WT using a doubly fed induction generator (DFIG) [35]. The MPPT was accomplished by applying control to the generator speed and blade pitch angle. The parameters of the FLC are optimized by using a genetic algorithm (GA). Initial simulation results prove that the proposed MPPT algorithm possesses good dynamic and steady state performances under different operating conditions.

In a wider field also related to wind turbines, Adedeji et al. study the optimization of the hyperparameters of the machine learning models in wind turbines [36]. It is applied to condition monitoring. The performance of different evolutionary algorithms is shown. The same problem is addressed in [37], where the operating condition of Kaplan turbine bearings was investigated by vibration diagnostics.

Nevertheless, although there are some studies that develop pitch controllers using artificial intelligent techniques, works that combine a gain scheduling fuzzy logic control scheme optimized with genetic algorithms and lookup table, and that also consider reducing the fatigue, are scarce in the literature.

3. FOWT Power Equations

The power P (W) generated by the wind in a wind turbine is determined by the following equation [38]:

$$P = 0.5\rho A v_w^3, \tag{1}$$

where ρ is the air density (Kg/m^3), A is the area swept by the blades (m^2), and v_w is the wind speed (m/s). The maximum energy that can be extracted from the wind in a WT is theoretically determined by the Betz limit, which is 59% of the total wind energy. In order to obtain the real energy that a specific turbine can generate, it is necessary to know the power coefficient Cp. The Cp coefficient modifies the output power by the following relationship.

$$P = 0.5\rho A v_w^3 Cp(\theta,\ \lambda) \tag{2}$$

That is, Cp depends on the pitch angle of the blade, θ (rad), and the tip speed ratio (TSR), λ, and its value is unique for each turbine model. The relationship between the rotor tip speed and the wind speed is:

$$\lambda = \frac{\omega \cdot R}{v_w}, \tag{3}$$

where ω (rad/s) is the angular velocity of the rotor and R (m) is the effective radius of the blades.

To illustrate how the power coefficient $Cp(\theta,\ \lambda)$ varies with the pitch angle and the TSR, in Figure 1 the Cp curve of the NREL 5 MW FOWT used to validate our approach extracted from [39] is shown.

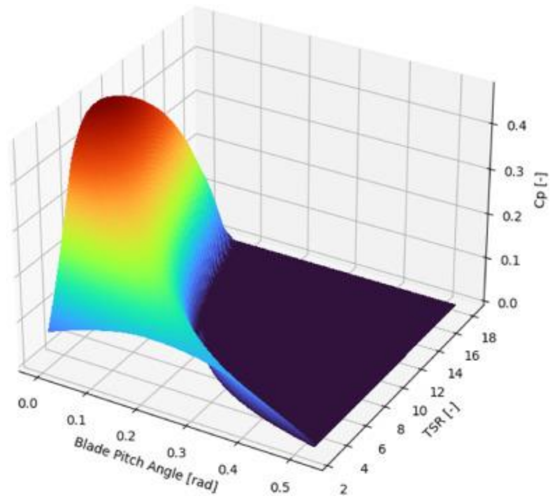

Figure 1. Variation of the power coefficient with the pitch angle and the TSR for the NREL 5 MW wind turbine [39].

As observed, the curve has a different local maximum for each pitch angle. The value of the maximum decreases with the pitch angle, due to the fact that the surface of the blades that faces the wind is also reduced. In addition, when the pitch angle grows the local maximum appears with a lower TSR.

Wind turbines have four regions of operation, depending on the wind speed (Figure 2).

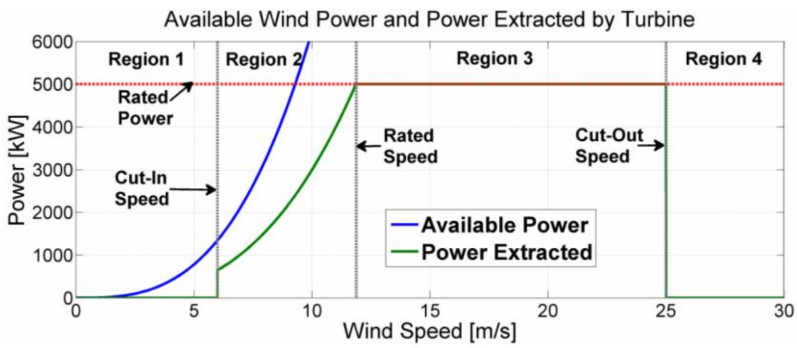

Figure 2. Wind turbine operation regions as a function of wind speed [40].

To maintain the rated power in region 3 (Figure 2), a control system is necessary in order to adjust the blade pitch angle, and to keep the power constant to its nominal value while wind speed increases.

To test the control proposal proposed here, the 5 MW NREL floating wind turbine, with ITI barge, has been simulated using FAST software. The main specifications of this FOWT are: rated wind speed, 12.1 m/s; blade length, 61.609 m; cut-out wind speed, 25 m/s; and nominal rotor speed, ω_{ref} 12.1 rpm [41]. The WT simulation model has been subjected to wind speeds within a range between 13 m/s and 21 m/s, and wave significant heights within a range from 1 m to 5 m.

4. Methodology

Variations of wind speed and wave significant height modify the operating point of the turbine and, as a consequence, the control is directly affected. A gain scheduling fuzzy controller (FLC) is proposed here. It allows coping with system nonlinearities and is capable of overcoming wind speed variations and turbulences. The aim of the gain scheduling algorithm is to ensure a correct operation for different wind and wave conditions. In addition, genetic algorithms (GAs) were used to optimize the controller over several operating points for different wind speeds and wave significant heights, so to build a lookup table of gains of the fuzzy controller.

The structure of the control system is shown in Figure 3. The control objective is to keep the output power at its rated value by controlling the collective pitch angle of the blades. In order to obtain the desired power output while minimizing turbine vibrations, fuzzy control is used as it allows determination of the control strategy without having to define a model of the dynamics of the FOWT [42]. Additionally, it has been shown to give a smooth response that does not add strong structure forces.

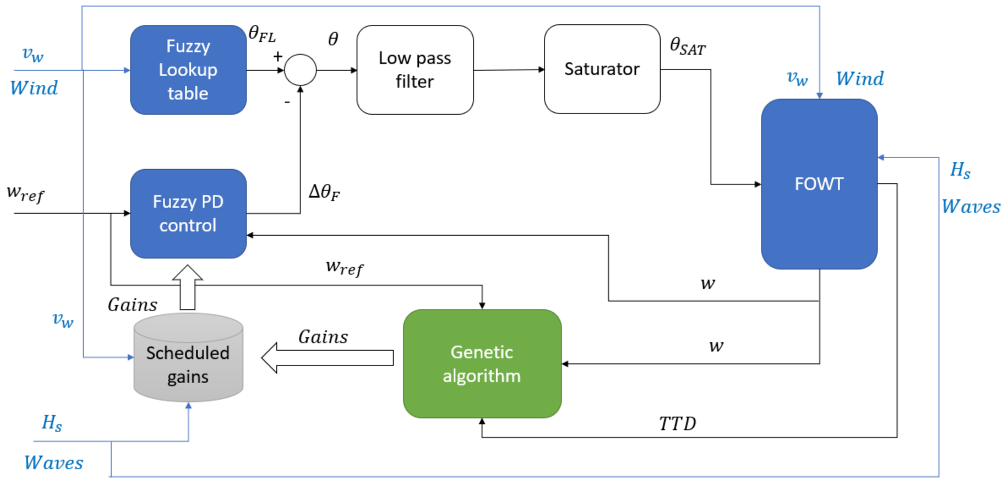

Figure 3. Hybrid intelligent controller with a fuzzy lookup table and a gain scheduling FLC tuned with GA.

The pitch control modifies the angle of the blades and is generally used to keep the output power at its nominal value, once the wind exceeds certain wind speed threshold, in region 3 (see Figure 2). On the other hand, controlling the angular velocity of the generator is typically used to track the optimal rotor speed (Cp) to maximize the output power when the wind is below that threshold, and thus the WT is working in region 2. In this work, we have focused on the pitch control. This actuator acts as a brake; when the wind speed is higher than the rate value, the pitch angle is increased in order to reduce the surface of the blades to the wind and thus, decelerate the rotor. This action contributes to maintaining the rotor speed and the output power around the nominal values. Depending on the rotor speed error, the pitch angle of the turbine is increased or decreased to maintain the desired rotor speed. If a greater rotor speed is demanded, the angle must be decreased, and vice versa, so as to keep the turbine operating in region 3.

The inputs of the fuzzy control system are: the current rotor speed, ω (rpm), and the rotor speed reference, ω_{ref} (rpm). The difference between them is the rotor speed error. A low-pass filter is designed to eliminate high-frequency oscillations in the control signal and to ensure that the frequency response of the controller is smaller than 0.2 rad/s. This is to avoid negative damping in the turbine response because the frequency response of the controller is 0.11 rad/s [41]. In addition, a saturator is added at the output of the controller to limit the signal to 25°, which is the maximum pitch angle for this type of turbine.

The fuzzy controller works with the rotor speed error, ω_e (rpm), defined in (4) and its derivative, $\dot{\omega}_e$ (rpm/s); both variables are normalized. The fuzzy controller is a Takagi–Sugeno type proportional derivative (PD), this is equivalent to a PI controller (5).

$$\omega_e = \omega_{ref} - \omega \tag{4}$$

$$\Delta u = f(\omega_e, \dot{\omega}_e) \tag{5}$$

The reference ω_{ref} is set to 12.1 rpm as it is the rated speed of the FOWT. For each of the two input variables, three membership functions are assigned, with triangular and trapezoidal shapes, with labels: positive, negative, and zero. The fuzzy rules are chosen based on experience, and are fine-tuned by trial and error, so that the controller output has the smoothest possible response without compromising controller performance.

The Takagi–Sugeno (TS) fuzzy rules are expressed as

$$Rule(i): \ if \ \omega_e \ is \ A_{1i} \ and \ \dot{\omega}_e \ is \ A_{2i} \ then \ \Delta\theta_{FL} = f_i(\omega_e \, , \, \dot{\omega}_e), \tag{6}$$

where A_{1i} and A_{2i} represent the membership functions of the inputs ω_e and $\dot{\omega}_e$, respectively, and the output variable y_i is the increment of the pitch angle calculated by the fuzzy controller, $\Delta\theta_F(^\circ)$. These fuzzy rules are as follows,

- If w_e is negative and $\dot{w}_e$ is negative, then $\Delta\theta_F$ is -5.
- If w_e is negative and $\dot{w}_e$ is zero, then $\Delta\theta_F$ is -2.5.
- If w_e is negative and $\dot{w}_e$ is positive, then $\Delta\theta_F$ is 0.
- If w_e is zero and $\dot{w}_e$ is negative, then $\Delta\theta_F$ is -2.5.
- If w_e is zero and $\dot{w}_e$ is zero, then $\Delta\theta_F$ is 0.
- If w_e is zero and $\dot{w}_e$ is positive, then $\Delta\theta_F$ is 2.5.
- If w_e is positive and $\dot{w}_e$ is negative, then $\Delta\theta_F$ is 0.
- If w_e is positive and $\dot{w}_e$ is zero, then $\Delta\theta_F$ is 2.5.
- If w_e is positive and $\dot{w}_e$ is positive, then $\Delta\theta_F$ is 5.

The total pitch angle that feeds the FOWT FAST model is obtained using the expression:

$$\theta = \theta_{FL} - \Delta\theta_F, \tag{7}$$

where θ_{FL} is the fuzzy lookup table output and $\Delta\theta_F$ is the fuzzy controller output. That is, the output of the fuzzy controller is used to correct the pitch angle calculated by the lookup table. This lookup table has also been implemented using fuzzy logic and emulates the relationship between wind speed and pitch angle provided by NREL in [41]. It interpolates the intermediate values using fuzzy rules. The input of the fuzzy lookup table, wind speed, is represented by three fuzzy sets: positive, negative, and zero; the output, as said, is the pitch angle of the blades, θ_{FL} (°).

A genetic algorithm (GA) has been used to tune the parameters of the incremental fuzzy PD controller. Genetic algorithms are computational methods for searching, learning, and optimization, loosely inspired by biological evolution. GAs are commonly used to generate high-quality optimization solutions, relying on biologically inspired operators such as mutation, crossover, and selection. Its configuration in this application is as follows. The size of the population is 50 individuals and they have been randomly initialized. Each individual has two chromosomes that correspond to tuning parameters GE and GDE of the FLC, that is, the gain of the error and of its derivative, respectively. The crossover probability has been set to 0.8 and the mutation rate is 0.05. Elite count has been set to 3. The creation function used is 'gacreationuniform'. The crossover function chosen is 'crossoverscattered'. The 'mutationgaussian' function has been implemented. Finally, the selection function was 'selectionstochunif'. All these functions are defined in the Global Optimization Toolbox of Matlab [43].

The cost function to be minimized by the genetic algorithm is given by

$$\begin{gathered} \overline{|\omega_e|} = \frac{\sum |(\omega_{ref} - \omega)|}{n}, \ \overline{|TTD|} = \frac{\sum |TTD|}{n}, \ \overline{\left|T\ddot{T}D\right|} = \frac{\sum \left|T\ddot{T}D\right|}{n}, \\ J = \sum \ \frac{\overline{|\omega_e|}}{\omega_{emax}} + \frac{\overline{|TTD|}}{TTD_{max}} + \frac{\overline{\left|T\ddot{T}D\right|}}{T\ddot{T}D_{max}}, \end{gathered} \tag{8}$$

where n is the number of samples of the simulation. The first term is used to minimize the mean absolute angular velocity error ($\overline{|\omega_e|}$); the second term aims to force the control action so as to reduce the amplitude of the fore–aft displacement of the tower top ($\overline{|TTD|}$), which is directly related to the loads on the turbine structure. The third term, $\overline{\left|T\ddot{T}D\right|}$, is included to reduce the acceleration of the tower, tackling the problem of the vibrations to which it is subjected, both by disturbances and by the effect of the control. These last two terms considered in an indirect way the effects of the wind speed and wave height. All these metrics are normalized by their maximum values to ensure they all contribute equally to the cost function. The GA stops when the best value does not change during the last 50 iterations.

The GA is run off-line to adjust the controller parameters. Once the GA ends, the best controller gains obtained per test case are stored in the table 'scheduled gains'. Each gain of the table corresponds to a specific wind speed, v_w, and wave height, H_S.

All parameters and variables mentioned previously are summarized in Table 1.

Table 1. List of parameters and variables.

Symbol	Name	Units
P	Output power	W
ρ	Air density	Kg/m^3
A	Area swept by the blades	m^2
R	Radius of the blade	m
$Cp(\theta, \lambda)$	Power coefficient	-
λ	Tip speed ratio	-
v_w	Wind velocity	m/s
ω	Rotor angular velocity	rad/s
ω_e	Angular velocity error	rad/s
ω_{ref}	Angular velocity reference	rad/s
θ	Pitch angle reference before saturation	deg
θ_{FL}	Pitch angle reference provided by the fuzzy lookup table	deg
$\Delta\theta_F$	Pitch angle reference obtained with the fuzzy PD controller	deg
θ_{SAT}	Pitch angle reference after saturation	deg
TTD	Fore–aft displacement of the tower top	m

5. Simulation Results and Discussion

The software OpenFast [44] developed by NREL was used to simulate the nonlinear floating wind turbine and the environmental disturbances; the hybrid intelligent controller was implemented with Matlab/Simulink software. The simulations were carried out with the IEC 61400-1 standard for load [45]. The proposed control approach is compared with the base controller BC embedded in FAST. Both controllers are evaluated regarding wind power extracted and vibrations, measured in terms of output power, vibration suppression rate η (9), and root mean square error ($RMSE$) (10).

$$\eta = \frac{\sigma_{GSFATS} - \sigma_{controller}}{\sigma_{GSFAST}} \cdot 100\%, \tag{9}$$

$$RMSE = \sqrt{\frac{\sum \left(y_{ref} - y\right)^2}{n}} \quad RMSE_N = \frac{RMSE_{controller}}{RMSE_{FAST}}, \tag{10}$$

where σ is the standard deviation of the WT oscillations, y_{ref} represents the reference signal, y is the output signal of FAST, and n is the number of samples. The metrics are obtained in both cases regarding the FAST controller, σ_{GSFAST}, which is taken as a reference. The normalized RMSE ($RMSE_N$) is calculated for the power output obtained in the turbine. The first 60 s are removed to eliminate the effect of transient response in the analysis [46].

5.1. Performance without Waves

First, the two controllers, the FAST baseline controller (BC) and the proposed one, fuzzy PI tuned by GA (AGFPI), are compared with a wind speed of 15 m/s and without waves. The simulation runs for 600 s to ensure that the results can be analyzed without transient effects.

Figures 4–8 show how the fuzzy controller (AGFPI, blue line) gives a faster response and lower amplitude oscillations compared to the controller included in FAST (BC, red line). This means that a smaller control effort is required and, thus, there is less degradation of the mechanical components.

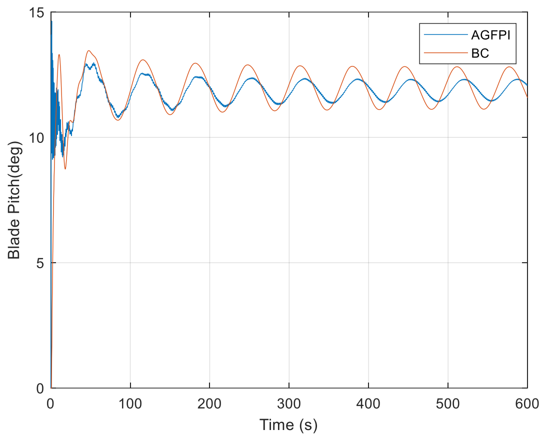

Figure 4. Pitch angle control without waves.

The rotor speed obtained with each controller is shown in Figure 5. It can be seen how both controllers are able to make the turbine work in the operating region 3, where they maintain the angular rotor speed around its nominal value, 12.1 rpm. However, the fuzzy controller (blue line) gives smaller oscillations.

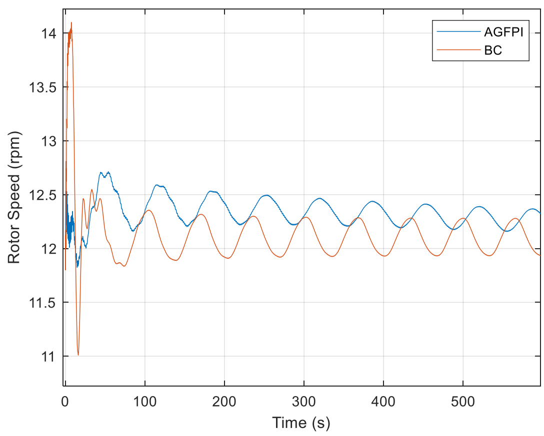

Figure 5. Rotor speed without waves.

The rated power of this floating wind turbine is 5 MW, therefore this is the target power. In Figure 6, it can be seen how both controllers are able to keep the power at the reference value. Again, the intelligent hybrid control system obtains an output power with smaller oscillations around the nominal value than the BC.

As mentioned before, the blade angle control also influences the stability of the FOWT. Two variables are used to analyze these effects: the pitch of the platform, θ_p (PtfmPitch), and the displacement of the tower top in the fore–aft direction (TTDspFA). The platform pitch indicates the angle (°) of inclination of the platform with respect to the horizontal axis, while the tower top displacement shows the linear downwind displacement (m) of the nacelle with respect to its equilibrium position. According to the FAST manual [47], the platform pitch is the degree of freedom that allows the platform to tilt around its reference point relative to the inertia frame. Thus, the pitch is calculated as a displacement that indicates the tilt rotation of the platform regarding its reference point. On the other hand, the TTDspFA is the tower top/yaw bearing fore–aft (translational) deflection (relative to the undeflected position). These measurements are shown in Figures 7 and 8, respectively, with both control strategies. In the figures on the left, the variables are represented in the time domain; on the right side of the figures their amplitude spectrum is shown.

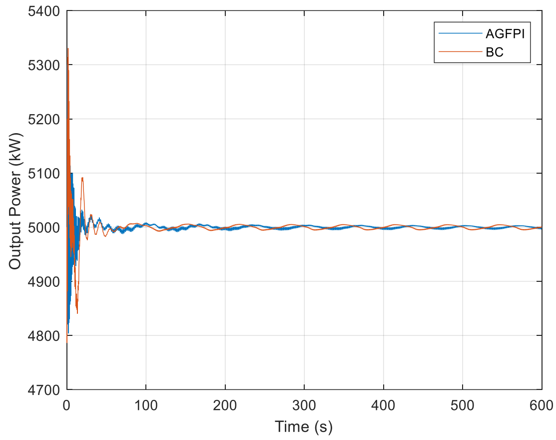

Figure 6. Output power without waves.

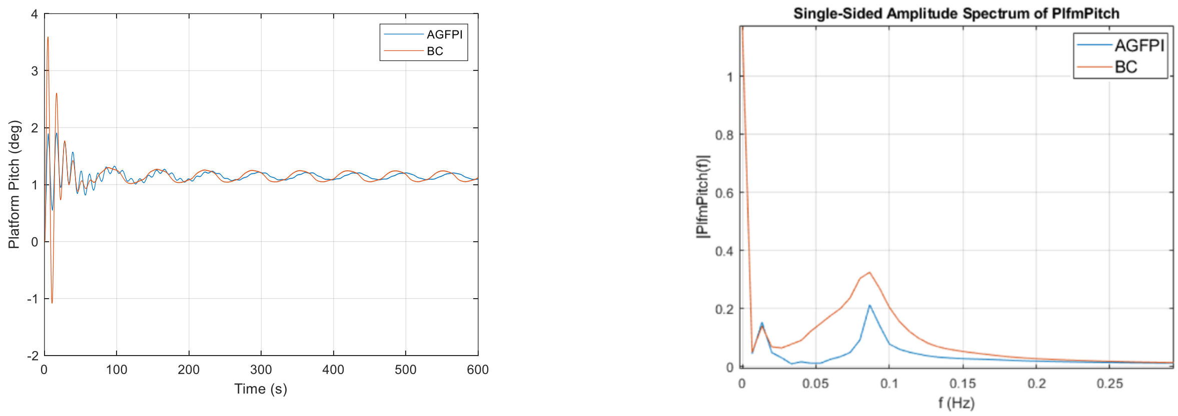

Figure 7. Platform pitch without waves (**left**) and its single side amplitude spectrum (**right**).

As shown in Figure 7, the BC controller generates larger oscillations for a longer time. In this sense, the fuzzy controller gives a slightly better response, particularly in the first 50 s. The amplitude spectrum (Figure 7, right) helps to corroborate the reduction in the amplitude of the oscillations with the intelligent hybrid controller. It is remarkable how the second mode is attenuated.

In Figure 8 (left), it is possible to observe that the displacement of the tower is initially much smaller with the proposed AG-fuzzy hybrid control. From the first 50 s on, both controllers provide a similar response though the fuzzy one is still a little better.

Figures 7 and 8 (right) show how the amplitude of the spectrum is reduced with the hybrid intelligent controller in comparison to the FAST controller. Indeed, the biggest reduction appears in the range of frequencies from 0.025 to 0.15 Hz. This confirms that for this simulation case, although the oscillation frequencies of the wind turbine are approximately the same, the amplitude is reduced for both the platform and the tower with the proposed controller.

In addition, the tower displacement spectrum (Figure 8, right) shows a small peak at high frequencies (around 0.58 Hz), which is not attenuated by any controller. This could indicate that the vibrations at that frequency come from the natural operation of the tower under these conditions. The fact that this peak does not appear in the platform may be due to the great mass and therefore the very high inertia of the barge.

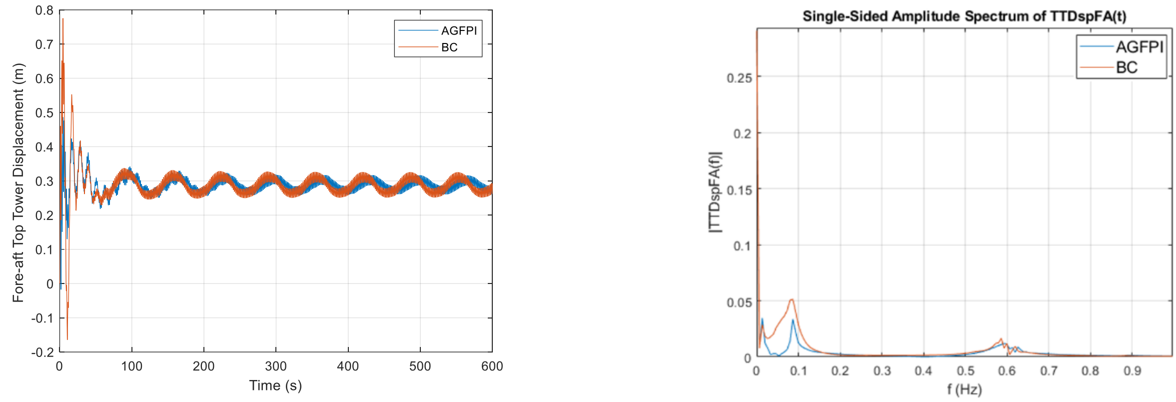

Figure 8. Tower top displacement in the fore–aft direction without waves (**left**) and its single side amplitude spectrum (**right**).

5.2. Performance with Waves

When working with offshore structures, it is very important to consider the effect that waves will have on them. In the following simulations, waves generated with the JONSWAP/Pierson–Moskowitz spectrum have been included. This spectrum is based on long measurements made in the North Atlantic Ocean [48] and is determined by Equation (11),

$$SWP(\omega_w) = \frac{5}{8}\pi H_s^2 \omega_{wp}^4 \omega_w^{-5} e^{-\frac{5}{4}\left(\frac{\omega_w}{\omega_{wp}}\right)^{-4}}, \tag{11}$$

where H_s is the significant wave height in m, defined as four times the standard deviation of the sea elevation; ω_{wp} is the peak angular frequency; and ω_w is the wave angular frequency, both in rad/s. The spectral density of the waves for H_s = 5 and ω_{wp} = 0.5067 is shown in Figure 9, left, and the corresponding wave elevation is depicted in Figure 9, right.

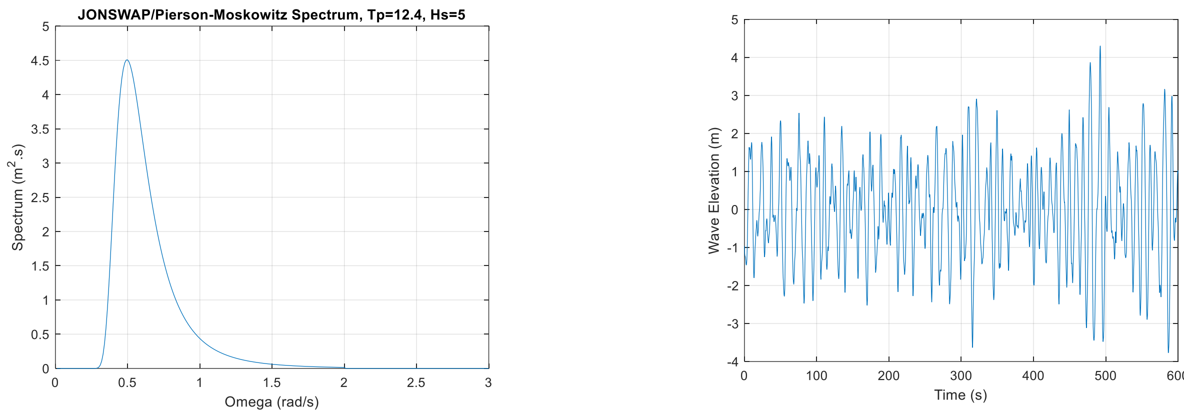

Figure 9. Wave spectral density (**left**) and wave elevation (**right**). H_s = 5, ω_{wp} = 0.5067.

In addition, we have simulated stochastic turbulent winds generated by the NREL TurbSim tool with average ranges from 13 m/s to 23 m/s, within region 3 of the floating 5 MW NREL wind turbine operation. The turbulence model uses the IEC standard with mean turbulence of 14 %. Figure 10 shows an example of wind profile with 17 m/s speed.

Different test cases have been carried out for different wave heights H_s, from 1 to 5 m; it is worth remarking that higher wind speeds are associated with higher wave heights. In all cases, the peak frequency of the wave spectrum is set to ω_{wp} = 0.5067 and it is maintained constant [49]. The software FAST is used to generate irregular waves following the described JONSWAP/Pierson–Moskowitz spectrum. The inclusion of waves in the simulation makes the control task more difficult because they are important disturbances for the system. Table 2 lists the test cases.

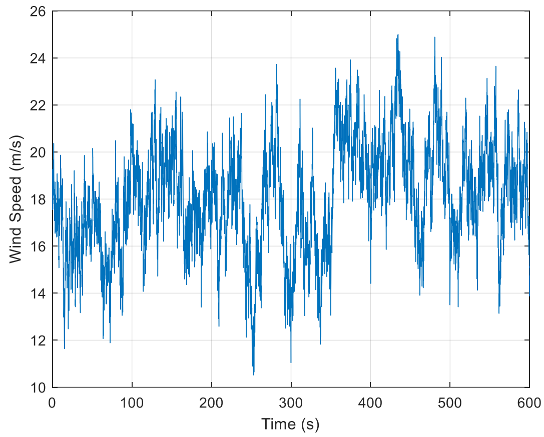

Figure 10. Random 17 m/s mean wind speed.

Table 2. Test simulation cases.

Test Case Number	Average Wind Speed (m/s)	Wave Height Hs (m)
1	13	1
2	15	2
3	17	3
4	19	4
5	21	5

The controller has been tuned for each test case and then evaluated with all the rest of the test cases, that is, with different environmental conditions. This allows us to study how generalizable are the results of the optimization, the robustness of the controllers, and the influence of the wind and wave conditions. Table 3 shows the value of the cost function (8) obtained during the evaluation. The column indicates the test case used to evaluate the performance of the controller and the row means the test case used to optimize the controller. As expected, the best results appear in the main diagonal of the table (these values have been boldfaced). In general, the cost function increases as we move away from the optimization conditions. The only exceptions appear in cells 3/5 and 4/1.

The best results are very similar each other; the difference between the maximum and the minimum is only around 5%. This fact indicates that the optimization process was able to tune the controller correctly regardless the weather conditions.

Table 3. Evaluation of the cost function for each test case.

Optimization Case/Test Case	Case 1	Case 2	Case 3	Case 4	Case 5
Case 1	**0.0958**	0.0989	0.1051	0.1106	0.1037
Case 2	0.1013	**0.0958**	0.0987	0.1194	0.1258
Case 3	0.1179	0.1088	**0.0947**	0.1104	0.1040
Case 4	0.1071	0.1082	0.0978	**0.0985**	0.1029
Case 5	0.1205	0.1185	0.1121	0.1085	**0.0999**

Figure 11 shows the results of the rotor angular speed in rpm (first row), the tower top displacement TTDspFA in m (2nd row), the platform pitch in degrees (3rd row), and the output power in kW (4th row) for the intelligent hybrid controller (AGFPI), in the left column, and for the FAST BC (in the right column) for test cases 1 (blue), 3 (red), and 5 (orange).

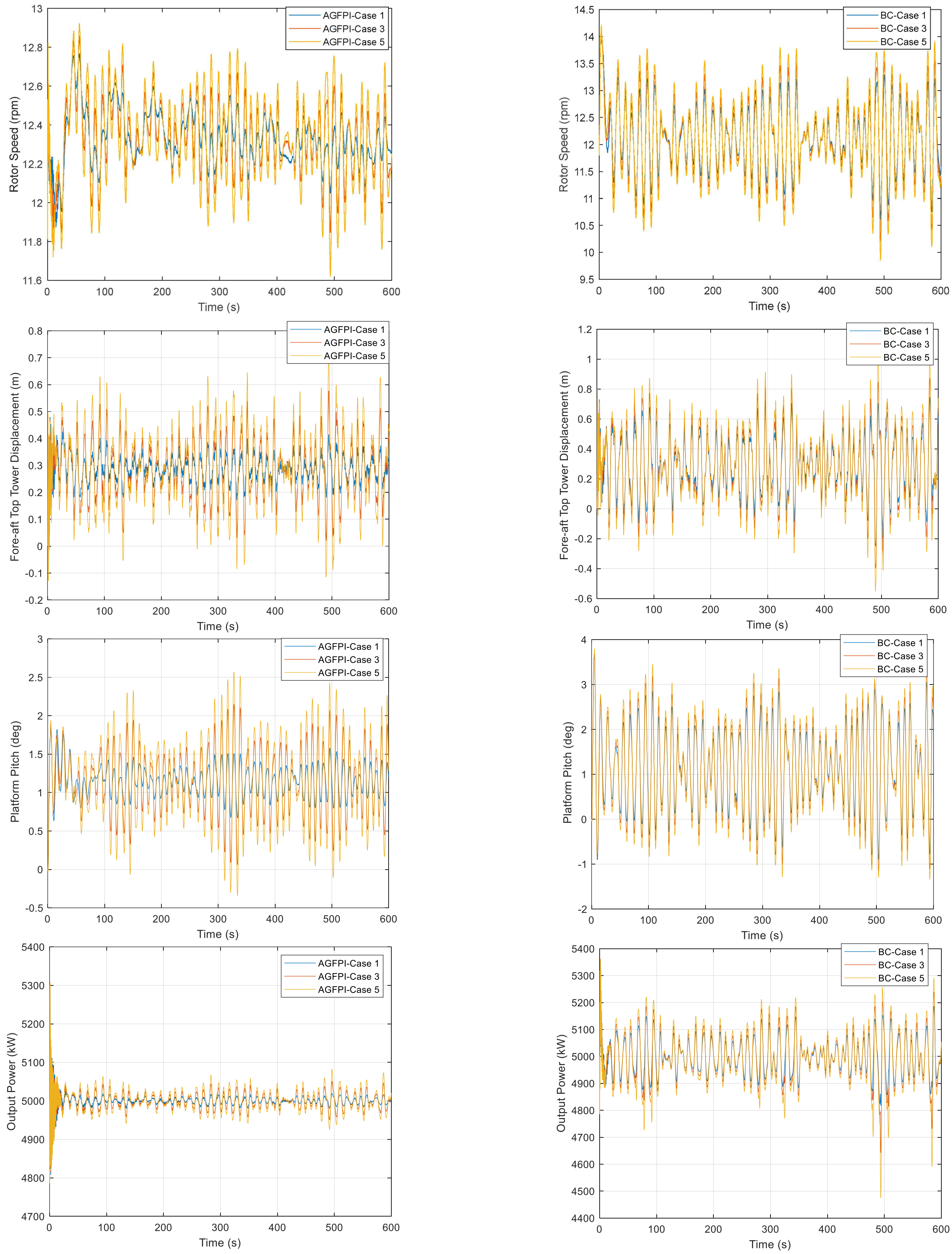

Figure 11. Simulations of tests cases 1, 3, and 5 using the intelligent hybrid controller (**left**) and the FAST controller (**right**).

In Figure 11, it can be seen how the proposed fuzzy logic controller provides a response with a smaller angular velocity error and lower oscillations, which means smaller loads for the turbine. When the AGFPI is applied, the rotor speed oscillates around the expected rate speed, that is, 12.1 rpm. However, with the BC the rotor speed average value varies much more and tends to be higher, slightly over 13 rpm. Moreover, the variation of the amplitude of these oscillations is larger. Regarding the second and third row, the tower top displacement and the platform pitch, respectively, the oscillations are also bigger when the BC is used, as corresponds to the rotor speed behavior. However, the frequency of the oscillations is similar in both cases. Another interesting result is that with the AGFPI, the vibrations are reduced but the power is not compromised. It is possible to observe how output power fluctuates correctly around the nominal power (fourth row). For the three cases analyzed, results are similar but, as expected, the amplitude of the oscillations increases with the wind speed and wave height. The control task becomes more complicated for both controllers, the hybrid one and the baseline controller.

Table 4 summarizes the suppression rate of the TTDspFA and the platform pitch, as well as the normalized RMSE of the power, obtained with the intelligent controller for all the test cases. It can be observed how the hybrid fuzzy controller obtains a relevant improvement by decreasing the platform and tower vibrations. These results represent a good range of improvement with respect to the BC embedded in FAST.

When the wind speed and wave height increase, the effects of the control action on the turbine in terms of structural stability are smaller compared to the disturbances of the wind and waves themselves. Therefore, the reduction of vibrations and, consequently, the loads on the turbine are less significant at higher wind speed and wave height. This explains why test case number 1 is the one with better performance in general (boldfaced).

Table 4. Controller performance with respect to TTDspFA and platform pitch.

Case Number	Suppression Rate (%) TTDspFA η_{x_t}	Suppression Rate (%) Platform Pitch η_{θ_p}	Normalized Power RMSE
1	**23.01**	**33.75**	**0.22**
2	10.22	25.32	0.39
3	5.25	15.34	0.58
4	7.10	19.21	0.49
5	6.92	19.31	0.41

Another interesting aspect to analyze in wind turbine control approaches is the fatigue [50]. A key parameter to measure the fatigue of any component of the structure is the damage equivalent load (DEL). In this work, the fatigue DEL of the FOWT blades with both controllers, the proposed AGFPI and the BC, is obtained with the objective of determining which controller presents better performance in terms of reducing the loads that affect the wind turbine. The classical rainflow counting technique [51] is used to estimate the DELs. This algorithm identifies the closed cycles in the stress–strain curve to estimate the loads on the turbine blades. The first 60 s have been removed to eliminate the effect of the transient response in the analysis. Results are shown in Table 5 (regarding the in-plane bending moment) and in Table 6 (with respect to the out-of-plane bending moment) of the blades.

Table 5. Controller performance with respect to the blade in-plane bending moment (fatigue DEL).

Case Number	Fatigue DEL AGFPI (kNm)	Fatigue DEL BC (kNm)	% Reduction
1	1387	1538	9.82
2	1465	1598	8.32
3	1412	1605	**12.02**
4	1556	1618	3.83
5	1565	1633	4.16

Tables 5 and 6 show how the loads exerted on the blades both in-plane and out-of-plane are lower when the intelligent hybrid logic controller is used. This fact is consistent with the results obtained in Table 4. As expected, when the wind or waves grow the fatigue increases.

Table 6. Controller performance regarding the blade out-of-plane bending moment (fatigue DEL).

Case Number	Fatigue DEL AGFPI (kNm)	Fatigue DEL BC (kNm)	% Reduction
1	5012	5237	**4.30**
2	5115	5266	2.87
3	5144	5301	2.96
4	5174	5322	2.78
5	5169	5313	2.71

In Table 5, it is possible to observe how for all the wind and wave scenarios considered, the damage equivalent load (DEL) is much lower when the proposed AGFPI controller is applied. The best improvement is obtained for case 3, where a 12.02% reduction is observed. The worst case occurs with case 4, where a 3.83% reduction is obtained. Still, in all the cases, a reduction of the fatigue is achieved with the proposed controller. Table 6 yields similar conclusions for all the cases tested. The DEL due to blade out-of-plane bending moment is much lower when the AGFPI control scheme is applied. The best improvement is obtained for case 1, where a 4.3% reduction is observed. The worst is case 5, with a 2.71% reduction.

In summary, as shown in the tables above, a relevant improvement in the fatigue DEL of the wind turbine is obtained with the proposed controller, which implies longer duration, less structural damage, and lower maintenance cost.

In general, the best results are obtained for the cases where the average wind speed is closer to the nominal wind speed of this type of turbine. This may be due to the fact that as the wind speed increases, the control task becomes more difficult and the external forces on the turbine also increase, further perturbing the system.

The results of this work will allow the implementation of FOWT controllers that, being an only system, are able to stabilize the power output while reducing the vibrations. The vibrations produce mechanical fatigue and deteriorate the turbine. Thus, the vibration damping provided by the proposed controller contributes to reducing the risk of damage, extending the useful life of the FOWT, and increasing the time between maintenance operations, which reduces the maintenance cost. Furthermore, it reduces the necessity of adding structural control devices to stabilize the WT.

6. Conclusions and Future Works

The control of floating wind turbines is more complex than for those installed on land due to the fact that they are massive, highly nonlinear systems, and above all because they are exposed to strong external loads due to wind, waves, and currents. In this work, an intelligent controller of a 5 MW barge-type FOWT has been designed. On the one hand, it is able to generate as much power as possible while maintaining the output power at its nominal value in the corresponding region of operation and, at the same time, it optimally adapts to different wind and wave conditions to reduce vibrations and structural damage.

The proposed control strategy is based on a fuzzy logic-based incremental PD controller with gain scheduling, combined with a fuzzy mapping function for wind speed. The FLC is optimized with genetic algorithms for different ranges of wind and waves. Control gains are stored in a database to ensure the controller is adjusted to those changes.

The results have been measured in terms of suppression rate of tower vibrations and oscillations of the platform, as well as the fatigue DEL of the blades. These results have been compared with the pitch controller embedded in the FAST software, which is used to simulate a realistic model of the floating turbine. Waves and winds with realistic magnitudes have been included to test the operation of the control strategies.

In most of the tested conditions, better power generation along with greater reduction in vibration and fatigue have been obtained with the intelligent hybrid control system compared to the one with FAST, producing a smoother response. Indeed, for all the wind and wave scenarios considered, the damage equivalent load (DEL) is much lower when the proposed AGFPI controller is applied. Regarding the fatigue related to the blade in-plane bending moment, the best improvement is obtained when the average wind speed is 17 m/s and the wave height is 3 m, with a 12% reduction. For the blade out-of-plane bending moment, the largest reduction in DEL is observed when the average wind speed is 13 m/s and the wave height is 1 m, the reduction being 4.3% more than the reference FAST controller.

Another interesting outcome is the suppression rate, that is, the reduction in the standard deviation regarding the results obtained by the baseline controller. For the tower top displacement, this suppression varies between 5% and 23%. This improvement is even better for the platform pitch as the suppression rate ranges from 15% to 33%.

As future work, it is proposed to test the controller on a small prototype, and to apply other intelligent techniques to improve controller performance such as reinforcement learning.

Author Contributions: C.S.: Conceptualization, Methodology, Software, Validation, Writing—Original Draft Preparation. M.S.: Conceptualization, Validation, Writing—Review and Editing, Supervision, Funding Acquisition. J.-E.S.-G.: Methodology, Formal Analysis, Supervision, Writing—Review and Editing. All authors have read and agreed to the published version of the manuscript.

Funding: This work has been partially supported by the Spanish Ministry of Science and Innovation under the project MCI/AEI/FEDER number RTI2018-094902-B-C21 and PDI2021-123543OB-C21.

Institutional Review Board Statement: Not applicable.

Informed Consent Statement: Not applicable.

Conflicts of Interest: The authors declare no conflict of interest.

References

1. Gomes, I.L.; Melício, R.; Mendes, V.M.; Pousinho, H.M. Wind power with energy storage arbitrage in day-ahead market by a stochastic MILP approach. *Log. J. IGPL* **2020**, *28*, 570–582. [CrossRef]
2. Javadinasab Hormozabad, S.; Gutierrez Soto, M.; Adeli, H. Integrating structural control, health monitoring, and energy harvesting for smart cities. *Expert Syst.* **2021**, *38*, e12845. [CrossRef]
3. Mikati, M.; Santos, M.; Armenta, C. Modelado y simulación de un sistema conjunto de energía solar y eólica para analizar su dependencia de la red eléctrica. *Rev. Iberoam. De Automática E Inf. Ind.* **2012**, *9*, 267–281. [CrossRef]
4. Villoslada, D.; Santos, M.; Tomás-Rodríguez, M. General methodology for the identification of reduced dynamic models of barge-type floating wind turbines. *Energies* **2021**, *14*, 3902. [CrossRef]
5. Tomás-Rodríguez, M.; Santos, M. Modelling and control of floating offshore wind turbines. *Rev. Iberoam. De Automática E Inf. Ind.* **2019**, *16*, 381–390. [CrossRef]
6. Sierra-García, J.E.; Santos, M. Redes neuronales y aprendizaje por refuerzo en el control de turbinas eólicas. *Rev. Iberoam. De Automática E Inf. Ind.* **2021**, *18*, 327–335. [CrossRef]
7. Serrano-Barreto, C.; Santos, M. Intelligent fuzzy optimized control for energy extraction in large wind turbines. In *International Conference on Intelligent Data Engineering and Automated Learning*; Springer: Cham, Switzerland, 2020; pp. 269–276.
8. Jove, E.; González-Cava, J.M.; Casteleiro-Roca, J.L.; Alaiz-Moretón, H.; Baruque, B.; Leitão, P.; Pérez, J.A.M.; Calvo-Rolle, J.L. An intelligent system for harmonic distortions detection in wind generator power electronic devices. *Neurocomputing* **2021**, *456*, 609–621. [CrossRef]
9. Sierra-García, J.E.; Santos, M. Performance analysis of a wind turbine pitch neurocontroller with unsupervised learning. *Complexity* **2020**, *2020*, 4681767. [CrossRef]
10. Rahman, M.; Ong, Z.C.; Chong, W.T.; Julai, S.; Ng, X.W. Wind turbine tower modeling and vibration control under different types of loads using ant colony optimized PID controller. *Arab. J. Sci. Eng.* **2019**, *44*, 707–720. [CrossRef]
11. Song, Z.; Liu, J.; Hu, Y.; Cheng, Y.; Tan, F. Real-time performance analyses and optimal gain-scheduling control of offshore wind turbine under ice creep loads. *IEEE Access* **2019**, *7*, 181706–181720. [CrossRef]
12. Lemmer, F.; Yu, W.; Schlipf, D.; Cheng, P.W. Robust gain scheduling baseline controller for floating offshore wind turbines. *Wind. Energy* **2020**, *23*, 17–30. [CrossRef]
13. Wang, C.S.; Chiang, M.H. A novel pitch control system of a large wind turbine using two-degree-of-freedom motion control with feedback linearization control. *Energies* **2016**, *9*, 791. [CrossRef]
14. Christiansen, S.; Knudsen, T.; Bak, T. Extended onshore control of a floating wind turbine with wave disturbance reduction. In *Journal of Physics: Conference Series*; IOP Publishing: Bristol, UK, 2014; Volume 555, p. 012018.
15. Lemmer, F.; Schlipf, D.; Cheng, P.W. Control design methods for floating wind turbines for optimal disturbance rejection. In *Journal of Physics: Conference Series*; IOP Publishing: Bristol, UK, 2016; Volume 753, p. 092006.
16. Bagherieh, O.; Nagamune, R. Gain-scheduling control of a floating offshore wind turbine above rated wind speed. *Control Theory Technol.* **2015**, *13*, 160–172. [CrossRef]

17. Al-bayati, J.S.H.; Üstündağ, B.B. Hybrid intelligent technology for plant health using the fusion of evolutionary optimization and deep neural networks. *Expert Syst.* **2021**, e12756. [CrossRef]
18. Zouaidia, K.; Ghanemi, S.; Rais, M.S.; Bougueroua, L.; Katarzyna, W.W. Hybrid intelligent framework for one-day ahead wind speed forecasting. *Neural Comput. Appl.* **2021**, *33*, 16591–16608. [CrossRef]
19. Chen, Y.L.; Liu, Y.P.; Sun, X.F. The active frequency control strategy of the wind power based on model predictive control. *Complexity* **2021**, *2021*, 8834234. [CrossRef]
20. Djilali, L.; Badillo-Olvera, A.; Rios, Y.Y.; López-Beltrán, H.; Saihi, L. Neural high order sliding mode control for doubly fed induction generator based wind turbines. *IEEE Lat. Am. Trans.* **2021**, *20*, 223–232. [CrossRef]
21. Asgharnia, A.; Jamali, A.; Shahnazi, R.; Maheri, A. Load mitigation of a class of 5-MW wind turbine with RBF neural network based fractional-order PID controller. *ISA Trans.* **2020**, *96*, 272–286. [CrossRef]
22. Sierra-García, J.E.; Santos, M. Lookup table and neural network hybrid strategy for wind turbine pitch control. *Sustainability* **2021**, *13*, 3235. [CrossRef]
23. Dong, Y.; Zhang, H.; Wang, C.; Zhou, X. Wind power forecasting based on stacking ensemble model, decomposition and intelligent optimization algorithm. *Neurocomputing* **2021**, *462*, 169–184. [CrossRef]
24. Xie, J.; Zhang, H.; Liu, L.; Li, M.; Su, Y. Decomposition-Based Multistep Sea Wind Speed Forecasting Using Stacked Gated Recurrent Unit Improved by Residual Connections. *Complexity* **2021**, *2021*, 2727218. [CrossRef]
25. Sui, A.; Qian, W. Intelligent grey forecasting model based on periodic aggregation generating operator and its application in forecasting clean energy. *Expert Syst.* **2022**, *39*, e12868. [CrossRef]
26. Aparicio-Santos, J.; Hermosillo-Gómez, J.; Benitez-Pérez, H.; Alvarez-Icaza, L. Fuzzy controller to compensate comunication loads in real-time. *Rev. Iberoam. De Automática E Inf. Ind.* **2021**, *18*, 288–299. [CrossRef]
27. Escaño, J.M.; Sánchez, A.J.; Ceballos, M.; Gallego, A.J.; Camacho, E.F. Neuro-fuzzy estimator, with complexity reduction, of the temperatures of a parabolic-trough solar field. *Rev. Iberoam. De Automática E Inf. Ind.* **2021**, *18*, 134–145. [CrossRef]
28. Van, T.L.; Dang, N.K.; Doan, X.N.; Truong, T.H.; Minh, H.N. Adaptive fuzzy logic control to enhance pitch angle controller for variable-speed wind turbines. In Proceedings of the 2018 10th International Conference on Knowledge and Systems Engineering (KSE), Ho Chi Minh City, Vietnam, 1–3 November 2018; pp. 225–229.
29. Sierra-Garcia, J.E.; Santos, M. Deep learning and fuzzy logic to implement a hybrid wind turbine pitch control. *Neural Comput. Appl.* **2021**, *34*, 10503–10517. [CrossRef]
30. Kant, S.; Agarwal, D.; Shukla, P.K. A survey on fuzzy systems optimization using evolutionary algorithms and swarm intelligence. In *Computer Vision and Robotics*; Springer: Singapore, 2022; pp. 421–444.
31. Adedeji, P.A.; Olatunji, O.O.; Madushele, N.; Ajayeoba, A.O. Soft computing in renewable energy system modeling. In *Design, Analysis, and Applications of Renewable Energy Systems*; Academic Press: Cambridge, MA, USA, 2021; pp. 79–102.
32. Sahoo, D.K.; Sahu, R.K.; Sekhar, G.C.; Panda, S. A novel modified differential evolution algorithm optimized fuzzy proportional integral derivative controller for load frequency control with thyristor controlled series compensator. *J. Electr. Syst. Inf. Technol.* **2018**, *5*, 944–963. [CrossRef]
33. Borni, A.; Bechouat, M.; Bessous, N.; Bouchakour, A.; Zaarour, L.; Zaghba, L. Comparative Study of P&O and Fuzzy MPPT Controllers and Their Optimization Using PSO and GA to Improve Wind Energy System. *Int. J. Eng. Model.* **2021**, *34*, 55–76.
34. Sharma, S.; Tayal, V.K. Optimised controller design for frequency control of a wind turbine driven doubly fed induction generator. *Int. J. Ambient. Energy* **2022**, 1–10. [CrossRef]
35. Alaoui, C.; Saikouk, H.; Bakouri, A. MPPT Using Adaptive Genetic-Fuzzy Logic Control for Wind Power System. In *International Conference on Digital Technologies and Applications*; Springer: Cham, Switzerland, 2021; pp. 1787–1797.
36. Adedeji, P.A.; Olatunji, O.O.; Madushele, N.; Jen, T.C. Evolutionary-based Hyperparameter Tuning in Machine Learning Models for Condition Monitoring in Wind Turbines–A Survey. In Proceedings of the 2021 IEEE 12th International Conference on Mechanical and Intelligent Manufacturing Technologies (ICMIMT), Cape Town, South Africa, 13–15 May 2021; pp. 254–258.
37. Monkova, K.; Monka, P.P.; Hric, S.; Kozak, D.; Katinić, M.; Pavlenko, I.; Liaposchenko, O. Condition monitoring of Kaplan turbine bearings using vibro-diagnostics. *Int. J. Mech. Eng. Robot. Res.* **2020**, *9*, 1182–1188. [CrossRef]
38. Mikati, M.; Santos, M.; Armenta, C. Electric grid dependence on the configuration of a small-scale wind and solar power hybrid system. *Renew. Energy* **2013**, *57*, 587–593. [CrossRef]
39. López-Queija, J.; Robles, E.; Jugo, J.; Alonso-Quesada, S. Review of control technologies for floating offshore wind turbines. *Renew. Sustain. Energy Rev.* **2022**, *167*, 112787. [CrossRef]
40. Network, M.R.I. Report on physical modelling methods for floating wind turbines. *MARINET Rep.* **2015**. Available online: https://www.marinet2.eu/wp-content/uploads/2017/04/D2.20-Report-on-Physical-Modelling-Methods-for-Floating-Wind-Turbines-1.pdf (accessed on 10 November 2022).
41. Jonkman, J.; Butterfield, S.; Musial, W.; Scott, G. *Definition of a 5-MW Reference Wind Turbine for Offshore System Development (No. NREL/TP-500-38060)*; National Renewable Energy Lab. (NREL): Golden, CO, USA, 2009.
42. Civelek, Z.; Lüy, M.; Çam, E.; Mamur, H. A new fuzzy logic proportional controller approach applied to individual pitch angle for wind turbine load mitigation. *Renew. Energy* **2017**, *111*, 708–717. [CrossRef]
43. Global Optimization Toolbox, Matlab. 2022. Available online: https://es.mathworks.com/help/gads/getting-started-with-global-optimization-toolbox.html?s_tid=CRUX_lftnav (accessed on 10 November 2022).

44. NREL National Wind Technology Center" NREL.gov. Available online: https://www.nrel.gov/wind/nwtc.html (accessed on 10 November 2022).
45. IEC 61400-1. IEC 61400-1:2019 Wind Energy Generation Systems-Part 1: Design Requirements. 2019. Available online: https://www.une.org/encuentra-tu-norma/busca-tu-norma/iec?c=26423 (accessed on 10 November 2022).
46. Sarkar, S.; Fitzgerald, B.; Basu, B. Individual blade pitch control of floating offshore wind turbines for load mitigation and power regulation. *IEEE Trans. Control Syst. Technol.* **2020**, *29*, 305–315. [CrossRef]
47. Jonkman, J.M.; Buhl, M.L., Jr. *Fast User's Guide-Updated August 2005 (No. NREL/TP-500-38230)*; National Renewable Energy Lab. (NREL): Golden, CO, USA, 2005.
48. Moskowitz, L. Estimates of the power spectrums for fully developed seas for wind speeds of 20 to 40 knots. *J. Geophys. Res.* **1964**, *69*, 5161–5179. [CrossRef]
49. Li, Z.; Wen, B.; Dong, X.; Long, X.; Peng, Z. Effect of blade pitch control on dynamic characteristics of a floating offshore wind turbine under platform pitching motion. *Ocean. Eng.* **2021**, *232*, 109109. [CrossRef]
50. Mei, X.; Xiong, M. Effects of second-order hydrodynamics on the dynamic responses and fatigue damage of a 15 mw floating offshore wind turbine. *J. Mar. Sci. Eng.* **2021**, *9*, 1232. [CrossRef]
51. Downing, S.D.; Socie, D.F. Simple rainflow counting algorithms. *Int. J. Fatigue* **1982**, *4*, 31–40. [CrossRef]